

7. SEARCHING FOR NEW PHYSICS IN THE EXCLUSIVE $\gamma_{DELAYED} + \cancel{E}_T$ FINAL STATE

In this chapter we will present the results of the search in the exclusive $\gamma_{delayed} + \cancel{E}_T$ final state. Section 7.1 presents the results of the event selection outlined in Table 5.5 when applied to the 6.3 fb^{-1} data sample. We next use the data-driven background methods, described in Section 6.3, to estimate the number of events expected in the signal region ($2 \text{ ns} < t_{corr} < 7 \text{ ns}$) from SM and non-collision sources. In Section 7.2 we detail the results of the search and conclude that we find only a modest excess above background prediction. Section 7.3 compares this result to the 2008 result.

7.1 Event Selection and Background Predictions

Table 7.1 shows the event reduction from the full set of events collected by CDF to the final exclusive $\gamma + \cancel{E}_T$ event selection described in Table 5.5 before the final signal region timing requirement. We have 5,421 events passing all our event selection requirements and having a SpaceTime vertex which we will use to construct the t_{corr} timing distribution and look for evidence of $\gamma_{delayed} + \cancel{E}_T$. We also have 4,942 events which pass all the event selection requirements but have no SpaceTime vertex reconstructed (“no vertex sample”) which we will use to measure $\langle t_{corr}^0 \rangle$ as our estimate of $\langle t_{corr}^{WV} \rangle$. The timing distributions are shown in Figure 7.1 and 7.2 respectively.

As described in the background estimation procedure (Section 6.3), we begin by estimating the cosmic ray event rate for both the t_{corr} and t_{corr}^0 distributions. In Figure 7.1, we take the sample of events that have a SpaceTime vertex and look in the timing region between $20 \text{ ns} < t_{corr} < 80 \text{ ns}$. We fit a straight line in this region and use this to estimate the number of events from cosmic rays per nanosecond to

Event Selection	Number of Events
Pass Online/Offline Trigger selection with an identified photon w/ $E_T^0 \geq 45$ GeV and $\cancel{E}_T^0 \geq 45$ GeV	38,291
Pass Beam Halo Veto	36,764
Pass Cosmics Veto	24,462
Pass Track Veto for Tracks with $P_T > 10$ GeV	16,831
Pass Jet Cluster Veto for Jets with $E_T^0 > 15$ GeV	12,708
Pass Large $ Z $ Vertex Veto	11,702
Pass $e \rightarrow \gamma_{fake}$ Veto	10,363
Events with Good SpaceTime Vertex / No Reconstructed Vertex “ <i>Good Vertex Sample</i> ” / “ <i>No Vertex Sample</i> ”	5,421 / 4,942

Table 7.1

Event reduction table for the exclusive $\gamma + \cancel{E}_T$ search. The last selection requirement breaks the events into two samples: 1) Events that do have a reconstructed vertex and 2) Events that do not have a good SpaceTime vertex (“no vertex sample”). The sample of events that do have a reconstructed vertex are the events in which we perform our search for $\gamma_{delayed} + \cancel{E}_T$ while the “no vertex sample” is used to estimate the mean of the wrong vertex as described in Section 6.2.

be 32 ± 1 events. This rate is then used to predict the number of cosmic ray events we expect in the control and signal regions. Using Equation 4.3 we find:

$$N_{\text{SignalRegion}}^{\text{cosmics}} = 5 \text{ ns} \cdot \frac{32 \text{ events}}{\text{ns}} = 160 \pm 5 \text{ events} \quad (7.1)$$

Similarly, we perform a straight line fit from $20 \text{ ns} < t_{\text{corr}}^0 < 80 \text{ ns}$ for the no vertex sample to find the cosmics rate 38 ± 1 events per ns. We use a modified version of Equation 4.3 to find the cosmic rate in the region $-5 \text{ ns} < t_{\text{corr}}^0 < 3 \text{ ns}$:

$$N_{\text{NV}}^{\text{cosmics}} = \Delta T_{-5 \text{ ns} < t_{\text{corr}}^0 < 3 \text{ ns}} \cdot \frac{N_{\text{NVCosmicsRegion}}^{\text{cosmics}}}{\Delta T_{\text{CosmicsRegion}}} \quad (7.2)$$

$$N_{\text{NV}}^{\text{cosmics}} = 8 \text{ ns} \cdot \frac{38 \text{ events}}{\text{ns}} = 307 \pm 8 \text{ events.} \quad (7.3)$$

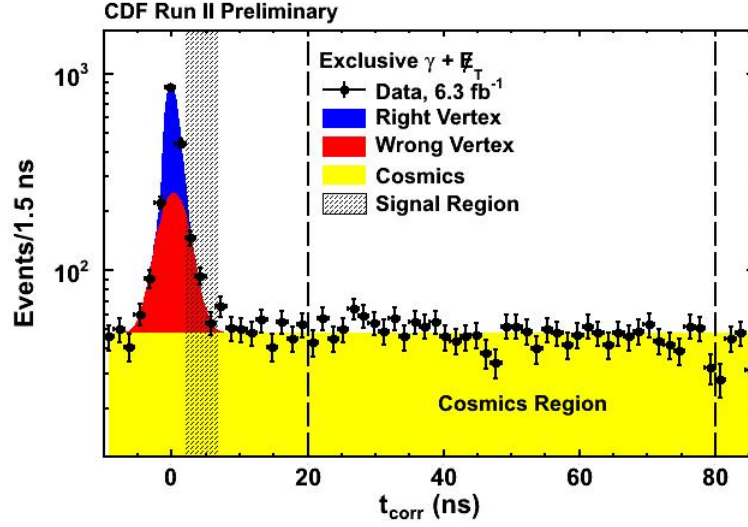


Fig. 7.1. The t_{corr} distribution for the final $\gamma + \cancel{E}_T$ dataset. In this plot we highlight the cosmics region, $20 \text{ ns} < t_{corr} < 80 \text{ ns}$, and use this to estimate the cosmic ray rate in the signal region $2 \text{ ns} < t_{corr} < 7 \text{ ns}$ as well as our control region as part of the background estimate procedure.

Using this we next perform a Gaussian plus straight line fit from $-5 \text{ ns} < t_{corr}^0 < 3 \text{ ns}$ with a fixed $\text{RMS} = 1.6 \text{ ns}$ to measure $\langle t_{corr}^0 \rangle$ as shown in Figure 7.2. We find $\langle t_{corr}^0 \rangle = 0.12 \pm 0.17 \text{ ns}$. The bottom of Figure 7.2 shows that the $\pm 1\sigma$ variation of the no vertex mean does describe the data well and thus gives us good confidence that this is a good measure of $\langle t_{corr}^0 \rangle$.

We estimate $\langle t_{corr}^{WV} \rangle = \langle t_{corr}^0 \rangle$ and conservatively overestimate a 100 ps systematic on the error of this prediction as described in Section 6.2. Using the estimation methods described in Section 6.3 and adding the uncertainties in quadrature we find $\langle t_{corr}^{WV} \rangle = 0.12 \pm 0.20 \text{ ns}$.

Finally we count the number of events in the bulk ($-2 \text{ ns} < t_{corr} < 2 \text{ ns}$) and control ($-7 \text{ ns} < t_{corr} < -2 \text{ ns}$) timing regions for the good vertex sample. The summary of the basic background estimation values and the breakdown of the number of observed events in the cosmics, bulk, and control region is given in Table 7.2.

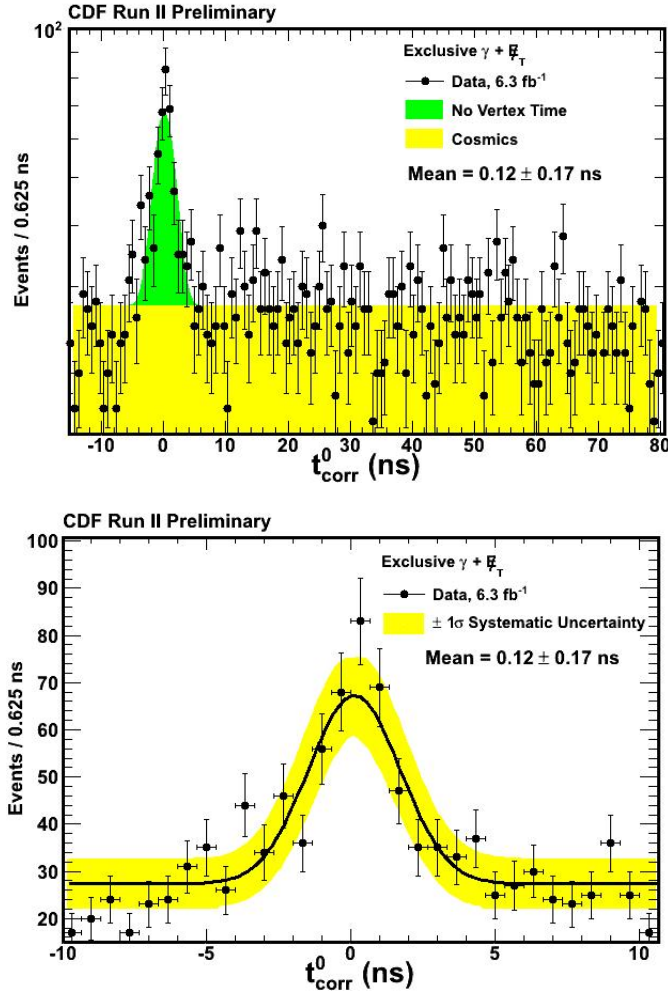


Fig. 7.2. (Top) The t_{corr}^0 distribution for the no vertex sample. Note that the straight line fit is performed in the cosmics region $20 \text{ ns} < t_{corr}^0 < 80 \text{ ns}$ and for the collision distribution a Gaussian is fit from $-5 \text{ ns} < t_{corr}^0 < 3 \text{ ns}$ with the RMS fixed to 1.6 ns while the mean of the Gaussian is allowed to vary in order to determine the best fit mean. (Bottom) Taking the $\pm 1\sigma$ systematic variation of the mean from the no vertex corrected time showing that $\langle t_{corr}^0 \rangle = 0.12 \pm 0.17$ ns well describes the distribution.

7.2 Results

Utilizing the estimation methods described in Section 6.3 and the results in Table 7.2 we can now predict the number of background events in the signal region.

Quantity	Measured Value	Error
No Vertex Mean	0.12 (ns)	± 0.17 (ns)
Cosmics per Nanosecond	32 (Events)	± 1 (Events)
Wrong Vertex Mean	0.12 (ns)	± 0.20 (ns)
Number of Events in the Cosmics Region <i>20 ns < t_{corr} < 80 ns</i>	1,919 (Events)	-
Number of Events in the Control Region <i>-7 ns < t_{corr} < -2 ns</i>	241 (Events)	-
Number of Events in the Bulk Region <i>-2 ns < t_{corr} < 2 ns</i>	1,463 (Events)	-

Table 7.2

Summary of the data-driven background measurements used for the exclusive $\gamma + E_T$ sample prediction.

Using Equation 3.11 we can compute the ratio of the number of events in the signal region to the number of events in the control region. From the mean of 0.12 ± 0.20 ns and Equation 3.10 we find a ratio of 1.20 ± 0.44 taking into account the uncertainty on the mean as well as the RMS. We predict the number of events from cosmic rays in the control region ($-7 \text{ ns} < t_{corr} < -2 \text{ ns}$) to be 160 ± 5 events using Equation 7.1. Taking the number of observed events in the control region from Table 7.2 minus the number of cosmics events we find

$$N_{Control}^{WV} = N_{Control}^{Obs} - N_{Control}^{Cosmics} = 241 - 160 = 81 \pm 17 \text{ events} \quad (7.4)$$

where we have ignored the right vertex contribution as it is expected to be less than 1 event in the control and signal timing region, and included the statistical

uncertainties on the measured values. To estimate the number of wrong vertex events in the signal region we take:

$$N_{Signal}^{WV} = R \cdot N_{Control} = 1.20 \cdot 81 = 96 \pm 35 \text{ events} \quad (7.5)$$

where we have taken into account the statistical uncertainties of the number of events observed as well as the uncertainties on R which is dominated by the uncertainty on the wrong vertex mean.

Combining the backgrounds, we find that

$$N_{Signal}^{Expected} = N_{Signal}^{WV} + N_{Signal}^{Cosmics} = 96 + 160 = 257 \pm 35 \text{ events.} \quad (7.6)$$

These results are summarized in Table 7.3. This procedure predicts that there are ~ 2 events from right vertex in the control and signal regions, well below the uncertainty of ± 35 events and thus is essentially negligible. The largest background in this final state comes from cosmic rays at almost a 2:1 ratio in the signal region. Meanwhile, our largest systematic uncertainty comes from the error on the wrong vertex mean which is dominated by the statistics of the events in the “no vertex” sample.

Quantity <i>(Events)</i>	Prediction <i>(Events)</i>
Number of Events from Cosmic Rays expected in the Signal Region	160 ± 1
Number of Events from Wrong Vertex expected in the Signal Region	96 ± 35
Total Number of Background Events Predicted in the Signal Region	257 ± 35
Total Number of Events Observed in the Signal Region	322

Table 7.3

Summary of the data-driven background prediction and observation for the exclusive $\gamma_{delayed} + \cancel{E}_T$ sample.

We now compare our background estimation to the data looking at the t_{corr} distribution shown in Figure 7.3 where we have used the 1,463 events in the bulk region and the methods in Chapter 3 to determine the total number of right vertex events. We observe 322 events in the signal region. To show how well the data is described, we compare the full background estimate and the data in the top of Figure 7.3 and the $\pm 1\sigma$ variation of the wrong vertex mean in the bottom of Figure 7.3. Figure 7.4 shows the background subtracted results where the yellow and green bands represent the $\pm 1\sigma$ and $\pm 2\sigma$ uncertainties in the systematics and the error bars on the data points represent the statistical uncertainties. We note that all errors were symmetrized in this plot for simplicity.

A modest excess remains in the data of observed minus predicted ($N_{Observed} - N_{Predicted}$) of 65 events in the signal region. While we note that the majority of the bins are above the expectations, we calculate the significance of this excess based purely on the results of the counting experiment. By taking into account both the systematic and the statistical uncertainty expected from the number of observed events in the data as part of the overall uncertainty we find:

$$\begin{aligned}
 N_\sigma &= \frac{N_{Observed} - N_{Predicted}}{\sqrt{\sigma_{N_{Pred}}^2 + \sigma_{N_{Obs}}^2}} \\
 N_\sigma &= \frac{322 - 257}{\sqrt{35^2 + 322}} \\
 N_\sigma &= 1.65
 \end{aligned}
 \tag{7.7}$$

An $N_\sigma = 1.65$ gives a one sided p-value (the estimated probability that this excess is inconsistent with a null hypothesis) of $\sim 5\%$. Since the standard for discovery in particle physics is considered 5σ (and for evidence is typically 3σ) we clearly cannot claim any evidence for new physics in our signal region, thus leading to the conclusion that we see no evidence for new physics in the exclusive $\gamma_{delayed} + \cancel{E}_T$ final state.

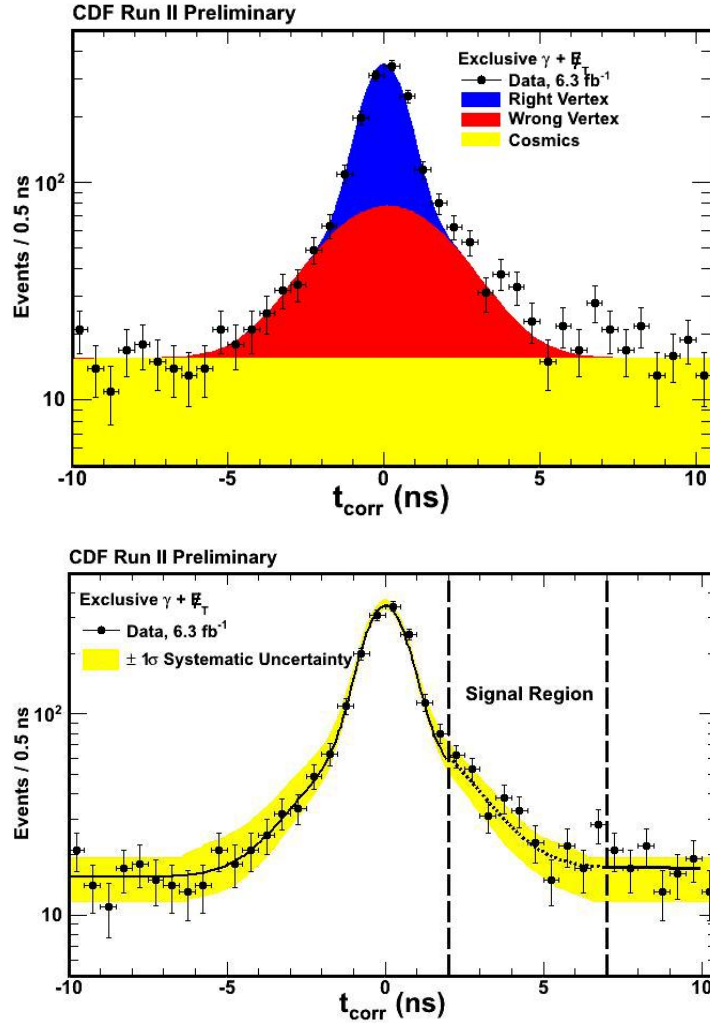


Fig. 7.3. (Top) The t_{corr} distribution of the $6.3 \text{ fb}^{-1} \gamma + \cancel{E}_T$ data showing the right, wrong vertex, and cosmics prediction. (Bottom) Taking the $\pm 1\sigma$ systematic variation of the mean of the wrong vertex showing that $\langle t_{corr}^{WV} \rangle = 0.12 \pm 0.20 \text{ ns}$ well describes the background distribution outside the signal region.

7.3 Comparison of the New Results with the Preliminary 2008 Results

The first question that arises following the results presented in Section 7.2 might be, “what happened to the excess shown in the preliminary 2008 result?”. As dis-

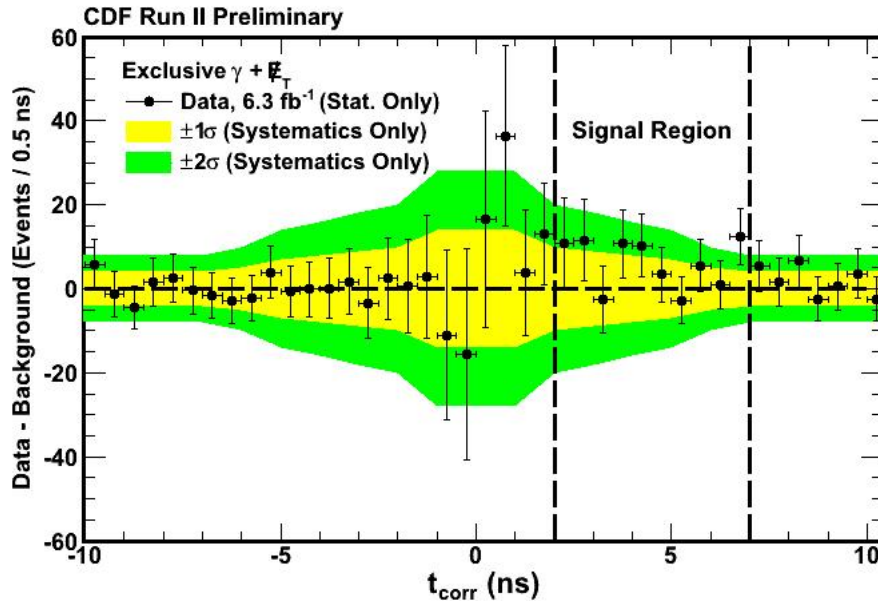


Fig. 7.4. The data minus background plot for the t_{corr} distribution where the yellow and green represent the $\pm 1\sigma$ and 2σ variation of the systematic and the error bars representing statistical error on the data. The events in the signal region correspond to a 1.65σ excess taking into account all the statistical and systematic uncertainties.

cussed in Section 1.6 an “excess” number of events above the background expectations of 67 events with a preliminary significance of $N_\sigma \sim 4$ was reported only using $\sim 4.77 \text{ fb}^{-1}$ of data. However, as we have learned, much of this excess was due to a poor background estimation technique, as well as due to sources of biased SM backgrounds in the sample. With the addition of numerous background rejection methods (Section 5.5), a more robust set of calibrations (Chapter 3), and a new data-driven background estimation procedure (Section 6.3) to predict the mean of the wrong vertex we now have an excess with a much smaller significance. While this provides a qualitative description, it is useful to make quantitative the difference between the previous analysis result and our current result. Asked differently, can we

tell which cuts made the difference and is there any evidence we made a real signal go away inappropriately?

We begin by listing the changes in the analysis which have taken place since the preliminary result in 2008. These changes are summarized in Table 7.4.

Change in Analysis	Impact on the Sample
Remove photon CES χ^2 requirement <i>Discussed in Chapter 2</i>	Add more events to our sample
Define photon ID relative to $z = 0$	Change the events in our sample
Add new cosmics veto: CES(E) and HAD(E) <i>Discussed in Chapter 4</i>	Remove events from our sample
Addition of data <i>Expand to 6.3 fb^{-1}</i>	Add more events to our sample
New calibrations procedure <i>Discussed in Chapter 3</i>	Changes the timing of the events
Change event E_T and \cancel{E}_T definition <i>Discussed in Section 5.5.1</i>	Change the events in our sample
Add large $ z $ vertex veto <i>Discussed in Section 5.5.3</i>	Remove events from our sample
Add $e \rightarrow \gamma_{fake}$ veto <i>Discussed in Section 5.5.2</i>	Remove events from our sample
New $\langle t_{corr}^{WV} \rangle$ estimation method	Changes the number of SM background events expected in the signal region

Table 7.4

List of changes and the impacted quantities in the analysis since the original 2008 $\gamma + \cancel{E}_T$ preliminary result.

- **Remove photon CES χ^2 requirement:**

Since the original analysis was done as a search for Large Extra Dimensions it included a selection on the CES χ^2 since this requirement aids in the reduction of jets that fake photons as well as cosmic ray candidates since the photon is assumed to come from the beamline. However, since it is known that this cut can be inefficient for photons that do not come directly from the beam line, for example, for use in searches for delayed photons which come from

the decay of some long-lived heavy object [38], we have elected to remove this requirement. The effect of this update is to allow more events into our sample some of which increase the jet background (although this is expected to be small since production rates for fake photons with more than 45 GeV is small) and some of which increases the cosmic rate. Additional cosmic ray rejection requirements are added later.

- **Define photon ID relative to $z = 0$:**

Another change to the photon definition includes a redefinition of the photon identification variables relative to $z = 0$ cm. Specifically, this effects the E_T^0 , energy isolation, track isolation, N3D track rejection, and 2nd CES cluster energy variables from Table 2.8 and discussed further in Appendix A. The overall effect of this update is to change the events that will be identified as having a “good” photon passing all our requirements. We note that despite including the E_T^0 variable in the photon identification, we still (at this point) select the events based on requiring $E_T^{vtx} > 45$ GeV and $E_T^{vtx} > 45$ GeV to distinguish between photon identification changes to the analysis and the impact of changing the E_T thresholds.

- **Add new cosmic veto: CES(E) and HAD(E)**

As discussed in Chapter 4, we also include the new cosmic rejection requirements into the photon identification variables. The addition of these requirements only reduce the total number of events that are present in our sample, specifically events likely to have originated from cosmic ray events.

- **Addition of data:**

Here we are simply adding data in order to update our result from the original 4.77 fb⁻¹ to 6.3 fb⁻¹ of data. The overall effect of this update should be to simply add more events to our sample.

- **New calibrations procedure:**

As discussed in Chapter 3, we include a new set of calibrations for the track t_0 as reported by the COT, the vertex t_0 as reported by the SpaceTime vertexing algorithm, and the photon t_f as determined by the EMTiming system. While this will change the number of events found in any one timing region, this will not effect the overall number of events in our sample.

- **Change event E_T and E_T^0 definition:**

As described in Section 5.4, the correlation between geometric and kinematic biases that come from the selection of an incorrect vertex leads to a migration of events into our sample with a large timing bias and out of the sample with a small timing bias. Therefore, we redefine our event selection to be $E_T^0 > 45$ GeV and $E_T^0 > 45$ GeV. This changes the number of events in the sample.

- **Add large $|z|$ vertex veto:**

Some of the most biased time events come from collisions that occur with $|z| > 60$ cm. As we showed in Section 5.5.3, these events have a large timing bias, and thus we veto them. The effect of this veto only reduces the number of events in our sample.

- **Add $e \rightarrow \gamma_{fake}$ veto:**

We implement the new $e \rightarrow \gamma_{fake}$ veto (described in Section 5.5.2). This veto is introduced in order to reduce the rate of events that enter our sample where an electron fakes a photon which are expected to have a large timing bias. The effect of this veto reduces the number of events in our sample.

- **New $\langle t_{corr}^{WV} \rangle$ estimation method:**

Finally, we use the new data-driven background estimation method, detailed in Chapter 6, to predict $\langle t_{corr}^{WV} \rangle$. While this does not change the number of

events in the sample, it does change our prediction of the number of expected events from SM sources in the signal region.

Now that we have a complete list of all the changes to the analysis we look to the impact of these changes to the number of events in the control and signal regions of the t_{corr} distribution. These results are summarized in Table 7.5. Since it is useful to quantify how much of the “excess” comes or goes because of an individual cut, we define the term “pseudo-excess” which is the number of events in the signal region minus the number of events in the control region. Said differently, it would be the excess if we used the old assumption of $\langle t_{corr}^{WV} \rangle = 0.0$ ns. While this doesn’t give a proper quantification because all the changes are correlated in the final analysis, and the order in which we present the changes matters, it does give a feel for the importance of each effect.

Sample	Number of Events in the Control Region	Number of Events in the Signal Region
Original $4.77 \text{ fb}^{-1} \gamma + \cancel{E}_T$ Sample (See Table 5.3) (w/ original E_T and \cancel{E}_T definitions)	124	191
Remove CES χ^2 requirement, apply new photon ID, and add cosmics veto	233	315
Add data	335	506
Apply new calibrations (See Chapter 3)	323	459
Redefine E_T^{Vtx} to E_T^0 (See Section 5.5.1)	315	453
Add large $ z $ veto (See Section 5.5.3)	267	375
Add $e \rightarrow \gamma_{fake}$ veto (See Section 5.5.2)	241	322
New $\langle t_{corr}^{WV} \rangle$ estimation method (See Chapter 6)	$241 \rightarrow 257 \pm 35$ expected	322

Table 7.5

Comparison of the new results against the original 2008 $\gamma + \cancel{E}_T$ preliminary result.

- **Updating the Photon Identification and Adding the Cosmics Rejection:**

As part of making our search more appropriate for a long-lived particle that decays to a photon we have removed the photon CES χ^2 (described in Section 2.4.3), applied the new photon identification requirements defined relative to $z = 0$ cm, and included of the new cosmics ray vetos (described in Section 4.2). We see an increase of 124 events in the signal region and 109 in the control region. This suggests an increase in the “pseudo-excess” from 67 to 82 events, which is reasonable since we have increased, overall, the number of events in the sample significantly. However, we must recall that at this point we have not taken into account many of the known biases (e.g. geometric biases, $e \rightarrow \gamma_{fake}$, large $|z|$ events, new calibrations, data-driven background prediction).

- **Add data:**

We now include the data up to 6.3 fb^{-1} and observe the number of events in the control region to rise to 335 and the number of events in the signal region to be 506. This is an increase of 191 events in the signal region and 102 in the control region and is in part due to additional luminosity as well as higher instantaneous luminosity affecting the rate at which cosmics enter the sample. This translates to an increase in the “pseudo-excess” from 82 to 171 events. This is the largest value we will see.

- **Apply new calibrations:**

The new calibration procedure calibrates using the event-by-event reconstructed time-of-flight rather than an assumed average time-of-flight. As seen in Table 7.5 this also has an effect of “reducing” the previously observed “pseudo-excess”. We observe after this change that there are 459 events in the signal region and 323 events in the control region, reducing the “pseudo-excess” of

from 171 events to 136 events. This result roughly implies that some 35 events of the “excess” were due to poorly calibrated vertex and/or EMTiming times.

- **Redefine E_T^{Vtx} to E_T^0 :**

When we apply the redefinition of E_T^0 and E_T^0 to our event selection we observe that the number of events in the signal region is reduced from 459 to 453 events in the signal region and from 323 to 315 events in the control region. This slightly adds to our “pseudo-excess” by raising it from 136 to 138 events. This implies that only a small fraction of the events, if any, in the signal region were a result of a kinematic selection bias.

- **Add large $|z|$ veto:**

As we can see from Table 7.5, after applying the large $|z|$ veto we are left with 375 events in the signal region and 267 events in the control region. This is a reduction of 78 and 48 events respectively, reducing the “pseudo-excess” from 138 to 108. To help further illustrate the impact of this veto we examine the events that fail the large $|z|$ veto but pass all the other requirements. Figure 7.5 shows the timing distribution for events that pass all the selection requirements in Table 5.5 up to the large $|z|$ vertex veto (i.e., without the $e \rightarrow \gamma_{fake}$ veto), but where we require the event to fail the large $|z|$ veto and have a good SpaceTime vertex. The shape of the double Gaussian suggests that the overwhelming majority of the events originate from wrong vertex events. The mean of the wrong vertex distribution is found to be shifted to 1.4 ns. While these events could have been rejected by the $e \rightarrow \gamma_{fake}$ veto, it is clear that if left in our final sample this shift in the wrong vertex distribution would introduce a large timing bias and thus contribute to events in the signal region from SM sources.

- **Add $e \rightarrow \gamma_{fake}$ veto:**

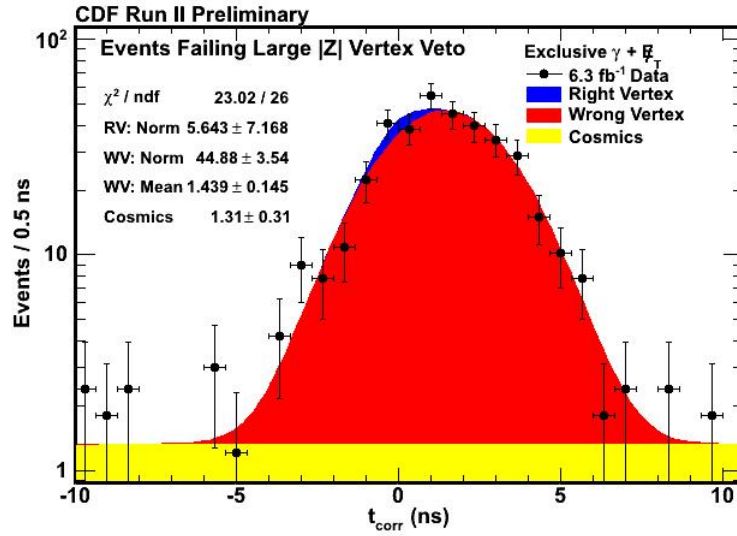


Fig. 7.5. The t_{corr} distribution for the exclusive $\gamma + \cancel{E}_T$ events that pass all the selection requirements in Table 5.5 but fail the large $|z|$ veto and where no $e \rightarrow \gamma_{fake}$ veto is applied and we require a good SpaceTime vertex. These events have a clear bias to large t_{corr} times with 78 events between $2 \text{ ns} < t_{corr} < 7 \text{ ns}$ and 48 events between $-7 \text{ ns} < t_{corr} < -2 \text{ ns}$ and thus contributed to the excess seen in the preliminary study done in 2008.

After applying the $e \rightarrow \gamma_{fake}$ veto we arrive back at our original number of 322 events in the signal region and 241 events in the control region which is a reduction of 53 events in the signal region and 26 events in the control region; shrinking the “pseudo-excess” from 108 to 81. Figure 7.6 shows the t_{corr} timing distribution for events that pass all the selection requirements in Table 5.5 up to the $e \rightarrow \gamma_{fake}$ veto, but failing the $e \rightarrow \gamma_{fake}$ veto and then requiring these events to have a good SpaceTime vertex. These events are likely coming from $W \rightarrow e\nu \rightarrow \gamma_{fake} + \cancel{E}_T$ and have a mean time of $\sim 0.5 \text{ ns}$. It is clear that the inclusion of this new veto further reduces SM events in the signal region as expected and contributed to the excess in 2008.

- **New $\langle t_{corr}^{WV} \rangle$ estimation method:**

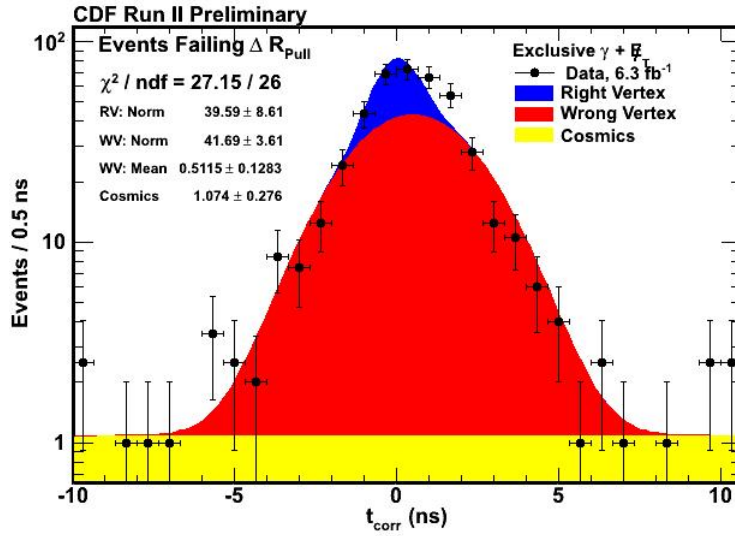


Fig. 7.6. The t_{corr} distribution for the exclusive $\gamma + \cancel{E}_T$ events that pass all the selection requirements in Table 5.5 but fail the ΔR_{Pull} veto. These events, likely coming from $W \rightarrow e\nu \rightarrow \gamma_{fake} + \cancel{E}_T$, have a clear bias to large t_{corr} times with 53 events between $2 \text{ ns} < t_{corr} < 7 \text{ ns}$ and 26 events between $-7 \text{ ns} < t_{corr} < -2 \text{ ns}$ and thus contributed to the excess seen in the preliminary study done in 2008.

Figure 7.7 shows the t_{corr} distribution for the final 6.3 fb^{-1} result where the background estimation method assumes $\langle t_{corr}^{WV} \rangle = 0 \text{ ns}$. The comparison with Figure 7.3 allows us to show how using the incorrect assumption that the $\langle t_{corr}^{WV} \rangle = 0 \text{ ns}$ can lead to the errant t_{corr} conclusion of an excess number of events in the signal region ($2 \text{ ns} < t_{corr} < 7 \text{ ns}$). The proper background estimate changes the 241 events in the control region to a proper background estimate of 257 events. We thus go from a “pseudo-excess” from 81 events to an excess of 65 events clearly indicating that part of the excess seen in 2008 was from mis-modeling of the background.

With all this in mind, in the next chapter we summarize the results of this search, describe how future versions of this analysis may gain sensitivity, and outline how to quantify our sensitivity to new physics models.

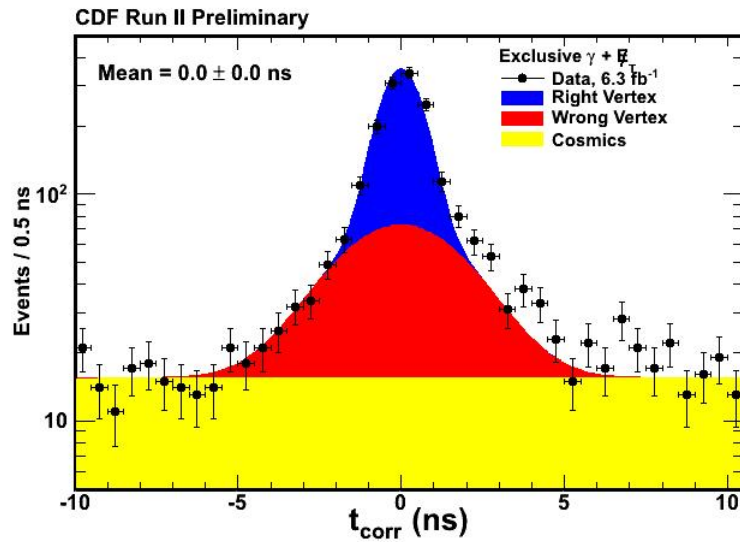


Fig. 7.7. The t_{corr} distribution for the final exclusive $\gamma + \cancel{E}_T$ but where we assume $\langle t_{corr}^{WV} \rangle = 0$ ns in the background estimate. This is to be compared to Figure 7.3 where we find $\langle t_{corr}^{WV} \rangle = 0.12 \pm 0.20$ ns from our data-driven background estimation. This illustrates how this assumption can lead to the errant conclusion of an excess number of events in the signal region ($2 \text{ ns} < t_{corr} < 7 \text{ ns}$).